IL NUOVO CIMENTO **41 C** (2018) 182
DOI 10.1393/ncc/i2018-18182-8

COLLOQUIA: IWM-EC 2018

Constraints on the density dependence of the symmetry energy

J. ŁUKASIK(*) for the ASY-EOS and ASY-EOS II COLLABORATIONS
IFJ PAN - PL-31342 Kraków, Poland

received 3 December 2018

Summary. — Current status and future experimental plans for constraining the symmetry energy at supra-normal densities are presented. A special emphasis is put on significance of the results obtained by the ASY-EOS Collaboration in a broader astrophysical context, including the recent interpretations of the first LIGO and Virgo GW170817 gravitational-wave signal. The plans for a high-energy campaign at FAIR using the NeuLAND and the KRAB detectors will be outlined.

1. – Introduction

A lot of experimental and theoretical efforts have been made within more than a decade now to study the properties of the asymmetric nuclear matter. Despite the efforts, the underlying entity, the Equation of State (EoS) of nuclear matter remains still uncertain, especially beyond the saturation density. In general, the EoS relates the strength of the nucleon binding to the temperature, baryon density, ρ, and isospin asymmetry $\delta = (\rho_n - \rho_p)/\rho$ [1,2], where the subscripts n and p refer to the neutrons and protons, respectively. For a cold matter the EoS is usually split into a density-dependent symmetric matter contribution and a symmetry energy term proportional to the square of the asymmetry [3-5]:

$$E(\rho, \delta) = E(\rho) + E_{sym}(\rho)\,\delta^2. \tag{1}$$

The latter describes solely the dependence of the EoS on asymmetry and is of high importance for both, the nuclear physics and the astrophysics. Possible higher-order terms with even powers of δ have been neglected here. The problem has been attacked experimentally from three sides: by performing the astrophysical and astronomical observations, by measuring the observables related to the nuclear structure, and by investigating the density and asymmetry dependent processes in heavy-ion collisions. The nuclear and

(*) E-mail: jerzy.lukasik@ifj.edu.pl

astrophysical sources are expected to provide coherent results despite their almost 19 orders of magnitude difference in scale. After all, they are driven by the same nuclear interactions. But, how is it in reality?

Significance of the quest for the EoS is reflected by the amount and the scales of the on-going and planned projects. The quest became not only multi-disciplinary but also a multi-messenger one, especially on the astronomy and astrophysics side. Here, the astrophysical objects and processes are observed using photons from radio waves through X-rays to gamma rays, neutrinos, cosmic rays and gravitational waves. It is only recently that the ultra-high-precision interferometers started to register the gravitational wrinkles due to the neutron star, NS, merger events [6] and that the LISA Pathfinder [7] mission demonstrated that a space-based observatory of gravitational waves is within our technical reach and can be operational around 2030. It is also only last year that the NICER [8] X-ray space observatory started its mission at the ISS. The mission aims at accurate mass and radius measurements of several NS through precise time-resolved X-ray spectroscopy. Such data should allow to precisely pick the corresponding EoS and pin down the associated symmetry energy. The mission is supposed to operate for 18 months. Taking into account that the predicted most probable rates for detection of binary NS mergers with the advanced LIGO detectors are 10–500 events per year [9], one can expect a rapid progress in constraining the high density EoS from the astrophysical sources in the nearest future.

The terrestrial laboratory investigations of the high-density asymmetric nuclear EoS become multi-messenger as well. The latest high-energy experiment, carried out in 2016 at RIKEN by the SPiRIT Collaboration [10,11], aims at extracting the symmetry energy by combining the information on charged-pion production rates, proton and neutron elliptic flows and possibly also on light isobar flows. Some very preliminary results have already been presented this year [12-14]. The results of the two earlier high-energy experiments: the FOPI-LAND measurement [15] reanalyzed by Russotto *et al.* [16] and the ASY-EOS measurement [17] will be discussed below in a broader context. Awaiting for the beams from the upcoming FAIR facility a proposal by the ASY-EOS II Collaboration of a new-generation experiment will be presented.

2. – Symmetry energy

The symmetry energy, E_{sym}, accounts for an excess of the nucleon binding in a pure neutron matter with respect to a symmetric matter (the one with equal numbers of neutrons and protons) at the same density. It is usually expressed in the form of a Taylor expansion (2) around the normal density $\rho_o \simeq 0.16\,\mathrm{fm}^{-3}$:

$$E_{sym}(\rho) \simeq E_{sym}(\rho_o) + \frac{L}{3}\left(\frac{\rho-\rho_o}{\rho_o}\right) + \frac{K_{sym}}{18}\left(\frac{\rho-\rho_o}{\rho_o}\right)^2 + \cdots \tag{2}$$

where L and K_{sym} are the slope and curvature parameters at ρ_o and together with the value of the symmetry energy at ρ_o, the $E_{sym}(\rho_o)$, they form a set of the main unknowns of the symmetry energy. Apart from the higher order parameters there are, however, also other quantities that enter a more exact parametrization of the E_{sym} at the mean-field level when its momentum dependence is taken into account [18]. They appear in the form of effective masses which, in principle, can be different for neutrons and protons. The E_{sym} is usually also split into its kinetic and potential parts, where the former is expressed using the isoscalar effective mass which may be an additional source of uncertainty.

3. – Why so important?

The density dependence of E_{sym} is an important ingredient for evaluating the drip lines, masses, density distributions and collective excitations of neutron-rich nuclei in nuclear structure studies [19,20], flows, fragment and particle production rates and multi-fragmentation in heavy-ion collisions [5, 21], and also for simulations of astrophysical processes like supernovae, stellar nucleosynthesis and objects like neutron stars [22].

In astrophysics the EoS in the density range 1–3 ρ_o plays an essential role in modeling the interiors of the NS [4]. It is still poorly known in this range of densities but uniquely determines the relation between their mass and radius, proton fraction, moment of inertia, crust-core transition. Matter that is less susceptible to compression (described by a so-called stiff EoS) will favor larger NS for a given mass. Such an EoS also predicts larger values for the maximum mass of a NS that can stand the gravitational collapse into a black hole. On the other hand, easily compressible matter (corresponding to a soft or super-soft EoS) will allow for smaller radii and smaller threshold masses. As will be shown later, the current constraints on the E_{sym} allow for a still rather broad variation of the NS radii: from ∼10 to ∼ 14 km.

4. – Why so uncertain?

On the theory side the uncertainties arise, among others, from the fact that the parameters of the phenomenological forces are being fixed around the saturation density and for nearly symmetric matter while the extrapolations above ρ_o and for neutron-rich or pure neutron matter have still a broad range of freedom. At high densities the many-body interactions begin to play a role and here the uncertainties regarding their strength and isospin dependence become noticeable. These and other deficiencies [23-26] result in a broad spectrum of predictions for the nuclear EoS, even of those resulting from the *ab initio* calculations, which are claimed to be parameter free. Especially the E_{sym} shows very different behaviors, in particular at supra-normal densities, calling for more tight experimental constraints at high densities.

But, on the experimental side the situation is even more dramatic, because no matter how precise the measurement is, extraction of the E_{sym} parameters proceeds through some model inference and thus is model dependent. This kind of circular dependence might look frustrating, but in fact it is not, provided every other detail of the model, apart from the E_{sym}, is well under control. Thus constraining the symmetry energy becomes a very demanding task, requiring very high precision measurements and the state-of-the-art models. A very promising feature of the symmetry energy quest is that it is multi-disciplinary and becomes also a multi-messenger one. This guarantees a plenitude of complementary data from independent sources, which should overlap and finally converge.

In reality, the way towards convergence is not at all simple. Recent interpretations of the heavy-ion data on the pion production rates can be an example. Here, the FOPI data [27] on π^-/π^+ ratios have been relatively well described by three different models [28,29] and [30], leading however to quite incoherent conclusions as far as the stiffness of the E_{sym} was concerned. This confirms the importance of the efforts made by the transport model developers within the code comparison project [31] to perform thorough tests of the codes to identify their weak points and understand the discrepancies. Extraction of the EoS parameters from the astrophysical observations is not at all easier. Fortunately, the new precise data provide new constraints.

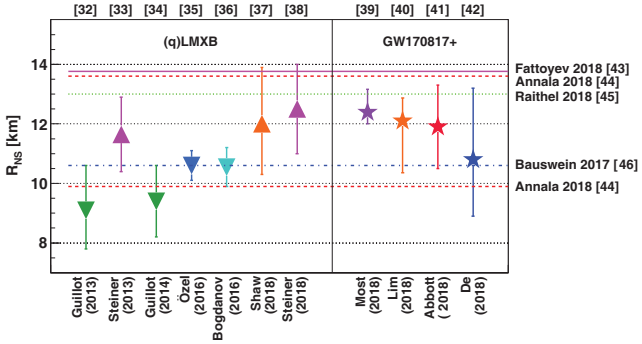

Fig. 1. – R_{NS} from different analyses of (q)LMXB and GW170817 (triangles and stars, respectively). The symbols correspond to refs. [32-42] from left to right. The lines represent the upper and lower limits from the early analyses of GW170817. They correspond to refs. [43-46] from top to bottom.

5. – Mass and radius of neutron stars from a "nuclear diesel"

From a simple consideration of a stellar object in a hydrostatic equilibrium one gets a dependence of the gradients of the pressure and of the mass shell on the density, thus two equations and three unknowns, all depending on the radius. In order to solve the problem one needs a third equation, the EoS, which relates these quantities. Thus the EoS of neutron-rich matter becomes indispensable for realistic NS simulations. Since there is a unique correspondence between the mass-radius relation and the EoS, it seems that measuring the masses and radii of NS should be sufficient to pick the right one. While precise mass measurements are possible especially for the radio and X-ray binary pulsars [47, 48], the measurements of the radii are more difficult and less accurate. Most promising for simultaneous mass and radius measurements (or inference) are the low-mass X-ray binary (LMXB) sources. These systems consist of an accreting NS and a lighter donor companion. In a more "explosive" class of binaries the NS accumulates the material until a critical density and temperature are reached causing the ignition of the fuel (mostly H and He). The fuel gets burned in a thermonuclear explosion within tens or hundreds of seconds. The bursts are separated then by hours or tens of hours of quiescence. From the measured energy and time structure of the associated X-ray bursts it is possible to infer the mass and radius of the NS [49, 50, 35]. This inference proceeds, however, through some assumptions (*e.g.*, about the composition of the NS atmosphere) and needs additional information like the temperature and distance to the source.

Recent measurements of the mass and radius of NS come mainly from the analyses of the thermal X-ray spectra from a more "static" class of LMXB, the transiently accreting binaries in quiescence (qLMXB). First analyses of the same five qLMXB from globular clusters gave however slightly inconsistent results for the NS radii: $R_{NS} = 9.1^{+1.3}_{-1.5}$ km [32] and $10.4 < R_{NS} < 12.9$ km [33] (the two leftmost points in fig. 1). The differences in radii may be due to different assumptions about the composition of the atmosphere, about the constancy of the radius for all NS, the distance uncertainty and different statistical inference methods. This dichotomy seems to persist up to now despite the subsequent reanalyzes including more qLMXB sources: $R_{NS} = 9.4 \pm 1.2$ km [34] or adding also thermonuclear bursters: $10.1 < R_{NS} < 11.1$ km [35], $9.9 < R_{NS} < 11.2$ km [36], $R_{NS} = 12^{+1.9}_{-1.7}$ km [37] and $11 < R_{NS} < 14$ km [38], see fig. 1.

6. – Gravitational-wave constraints

The first gravitational-wave signal from the neutron star merger event [6] has triggered immediately a lot of interpretations. We will focus on a few of them. The main constraint from the GW170817 event comes from the tidal deformability, Λ, which is related to the strength of the quadrupole mass deformation of a star due to the stress caused by its companion's gravity and obviously depends on the EoS. It was found to be $\Lambda < 800$ in [6]. This constraint together with the requirement that the EoS should support the $2\,\mathrm{M}_\odot$ neutron stars yielded the following limits for the radius of the $1.4\,\mathrm{M}_\odot$ NS: $9.9 < R_{NS} < 13.6\,\mathrm{km}$ in [44]. It very well matches the larger radius estimates from (q)LMXBs (see fig. 1). Reference [45] obtained the values of Λ for a few EoS supporting the R_{NS} values from 10 to 15 km. From the Bayesian inference the authors extracted the upper limit for the radius to be $R_{NS} < 13\,\mathrm{km}$ and the most likely one $R_{NS} \simeq 11.7\,\mathrm{km}$. GW170817 allowed also an estimate of the lower limit for the NS radius from the fact that the merger did not result in a prompt collapse, but instead some post merger electromagnetic emissions have been observed. This lower limit has been estimated to be $R_{NS} > 10.68\,\mathrm{km}$ in [46]. Extraction of tidal deformabilities for 10 relativistic mean field EoS taking into account the constraints from GW170817 allowed to estimate the upper limit for the radius to be $R_{NS} < 13.76\,\mathrm{km}$ in [43]. Here the L value has also been specified for the corresponding TAMUC-FSUa EoS: $L < 82.5\,\mathrm{MeV}$. The upper and lower limits from the above analyses are represented in fig. 1 by horizontal lines.

To complete the survey we quote the four most recent results constrained by the GW170817 event. Using a numerous family of the EoS and the Bayesian inference with the information on the lower and upper bounds on Λ as well as on the maximum mass of the NS, a most probable value of $R_{NS} = 12.39^{+1.06}_{-0.39}\,\mathrm{km}$ has been obtained in [39]. Similar analysis in [40] gave $R_{NS} = 12.10^{+0.77}_{-1.74}\,\mathrm{km}$. References [41] and [42] attempted at deriving more tight constraints on Λ than in the original report [6] by applying an additional condition on the maximum mass of the NS [48] and on the distribution of the measured masses. They arrived at the values of $R_{NS} = 11.9^{+1.4}_{-1.4}\,\mathrm{km}$ and $R_{NS} = 10.8^{+2.4}_{-1.9}\,\mathrm{km}$, respectively. These results appear as stars in fig. 1. They reveal a better agreement with the larger radius estimates from the binary X-ray systems.

7. – Squeezing the symmetry energy out of heavy-ion collisions

The increasing amount of experimental data on the parameters of the $E_{sym}(\rho)$ (53 have been collected in the most comprehensive review [51]) makes it more and more difficult to present them all together in a clear way. Since 2009 there have been several attempts to do so. Here, instead of quoting and discussing the individual results, we will show only the average values from the selected reviews to trace the progress (see fig. 2).

The first compilation of the data available in 2009 has been presented in [52]. It compares 7 results on the values of the $E_{sym}(\rho_o)$ and L parameters obtained from the isospin diffusion, neutron and proton yields, pygmy dipole resonances, PDR, and isobaric analogue states, IAS. The corresponding points in fig. 2 have been obtained in a similar way as those in ref. [53], *i.e.*, as simple mean values and average errors. The extracted mean values for $E_{sym}(\rho_o)$ and L amount to $31.06 \pm 0.83\,\mathrm{MeV}$ and $69.16 \pm 19.06\,\mathrm{MeV}$, respectively.

An update, including the results on binding energies, neutron skin thickness from the elastic polarized proton scattering and on electric dipole polarizabilities, EDP, as well as the results from the NS radius measurements was presented in ref. [54]. The extracted mean values amount to $32.14 \pm 0.93\,\mathrm{MeV}$ and $67.9 \pm 11.4\,\mathrm{MeV}$ in this case.

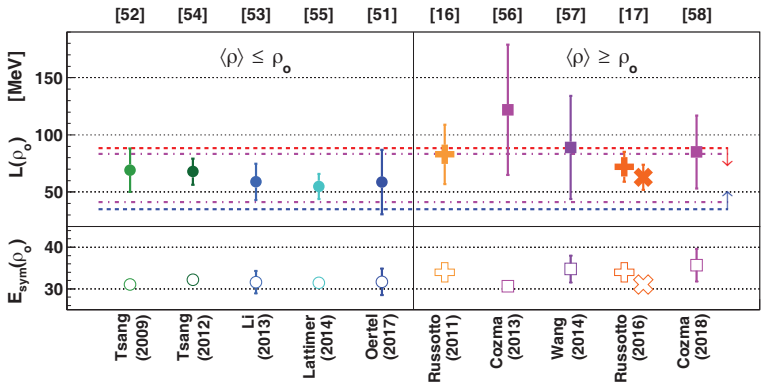

Fig. 2. – Average values of the $E_{sym}(\rho_o)$ (open symbols) and L parameters (filled ones) obtained from the compilations [52,54,53,55,51] (circles). The cross, refs. [16,17], and square, refs. [56-58], symbols represent the results obtained from the analyses of the FOPI-LAND and ASY-EOS data. The dashed lines represent the upper and lower limits for L converted from the R_{NS} limits obtained for the GW170817 event in [44] and [46], respectively. The dash-dotted lines represent the 2σ constraint from qLMXB [33].

The 28 results, including the analyses of atomic masses, isoscaling, IAS, skins, PDR, isospin diffusion, transverse flow, EDP, NS data compiled in [53] yielded the average values of 31.6 ± 2.66 and 58.9 ± 16.0 MeV for $E_{sym}(\rho_o)$ and L, respectively.

The analysis of correlations between L and $E_{sym}(\rho_o)$ for 6 observables: binding energies, neutron skin thicknesses, dipole polarizabilities, centroids of giant dipole resonances, isospin diffusion and IAS resulted in the overlap values of $E_{sym}(\rho_o)$ and L of 31.45 ± 1.05 MeV and 55 ± 11 MeV, respectively [55].

Finally the most extensive analysis [51] of 53 experimental results for $E_{sym}(\rho_o)$ and L yielded the average values of 31.7 ± 3.20 MeV and 58.7 ± 28.1 MeV, respectively.

These results have been presented as circles in the left part of fig. 2. All they have in common that they refer mostly to the observables sensitive to densities around or below the saturation density. Moreover, these experiments cannot claim to provide firm extrapolations to higher densities.

The only way to study the properties of the asymmetric nuclear matter at high densities in the laboratory conditions is to investigate the relativistic heavy ion collisions. The only two available so far results coming from the high energy experiments: FOPI-LAND [16] and the ASY-EOS [17], aiming at exploring the high density behavior of the E_{sym} are depicted in the right side of fig. 2 as cross symbols. They were obtained as the best fits of the model results to the experimental values of the elliptic flow ratios for neutrons and hydrogens as a function of the transverse momentum. The ratios have been obtained for the Au+Au collisions at 400 MeV/nucleon, at which the squeeze-out of the matter out of the reaction plane attains a maximum. The model that has been used here is the modified UrQMD version incorporating a power-law-like density dependence of the E_{sym} [59]. The values of L that have been obtained amount to 83 ± 26 and 72 ± 13 MeV for the [16] and [17] analyses, respectively, both obtained for $E_{sym}(\rho_o) = 34$ MeV. Lowering the $E_{sym}(\rho_o)$ value to 31 MeV in case of the ASY-EOS experiment resulted in a smaller value of $L = 63 \pm 11$ MeV (an $\times$ symbol in fig. 2). The figure shows also results obtained with other models describing the experimental flow ratios. The TüQMD model gave the value of $L = 122 \pm 57$ MeV for a fixed $E_{sym}(\rho_o) = 30.6$ MeV [56] when applied to the

FOPI-LAND data. Simulations performed with the same model but with a modified momentum dependent potential when compared to the ASY-EOS and FOPI/LAND results yielded a value of $L = 85 \pm 32\,\mathrm{MeV}$ for $E_{sym}(\rho_o)$ in the range $35.7 \pm 3.9\,\mathrm{MeV}$ [58]. An UrQMD model with various Skyrme forces [57] was able to best describe the FOPI/LAND data with the $L = 89 \pm 45\,\mathrm{MeV}$ for $E_{sym}(\rho_o)$ extracted from the Skyrme parameters in the range of $34.75 \pm 3.25\,\mathrm{MeV}$.

The dashed horizontal lines in fig. 2 represent the upper and lower limits for L obtained by converting the R_{NS} limits from the GW170817 event in [44] and [46], respectively. The approximate conversion has been done using the phenomenological pressure-radius relation from fig. 8 of [60]. The obtained L values for $R_{NS} = 13.6\,\mathrm{km}$ [44] and $R_{NS} = 10.68\,\mathrm{km}$ [46] amount to 88.5 and 34.9 MeV, respectively. The symmetry pressure, $p(\rho_o) = \rho_o L/3$. Finally, the dash-dotted lines represent the 2σ constraint on L from the qLMXB analysis of [33].

The high-density results are generally stiffer than the most recent averages from the low-energy experiments and from the nuclear data, which effectively probe densities below ρ_o. Most of them comply with the GW170817 constraint (within the precision of the $R_{NS} \to L$ conversion procedure) and also with the 2σ constraint from qLMXB [33]. On the other hand, the values of the symmetry energy constant from the analyses of the FOPI/LAND and the ASY-EOS data are generally higher than those from the systematics. This might partially account for the observed differences in L and be due to the correlation between the L and $E_{sym}(\rho_o)$ (see in particular the two results for [17], where the result for a reduced $E_{sym}(\rho_o) = 31\,\mathrm{MeV}$ (the $\times$ symbol in fig. 2) gets much closer to the recent averages for L). Nevertheless, since the high-energy experiments indeed have a chance to probe the densities above ρ_o, some differences might be expected.

The higher values of L from the high-energy experiments may support the hypothesis on the soft to stiff transition at supra-normal densities [23, 24]. Quantum Monte Carlo simulations of [23] predict that densities of up to $5\rho_o$ can be reached in the centers of the NS. Moreover, they predict that the uncertainty in the measured E_{sym} of $\pm 2\,\mathrm{MeV}$ may lead to an uncertainty as large as 3 km for the radius of the NS. These two predictions call for high-precision measurements of the symmetry energy at high densities (energies) to probe the EoS in the core of the NS and to provide the results relevant for astrophysics.

8. – ASY-EOS II @ FAIR (202?)

A future project aiming at improving the ASY-EOS results has to take into account two main goals: improvement of the precision, mainly through the usage of high-resolution detectors and radioactive beams, and extension of the density region probed, through the usage of high-energy beams. Microscopic simulations of [61] predict that the beams of energies around $\sim$1 GeV/nucleon should be sufficient to attain the densities of up to $\sim 3\rho_o$ in the central zone of a heavy-ion collision.

Simulations of semi-central Au+Au collisions at energies between 0.4 and 1.5 AGeV as well as neutron rich ^{132}Sn + ^{124}Sn and neutron poor ^{106}Sn + ^{112}Sn systems at 0.4–0.8 AGeV have been carried out by using the same version of the UrQMD transport code that has already been used in [17]. The neutron-to-proton elliptic flow ratio, $\mathrm{v2}_n/\mathrm{v2}_p$, at mid-rapidity ($0.4 < y_{lab}/y_{proj} < 0.6$), with a stiff and a soft parametrization of the potential part of the E_{sym} for semi central ($b_{red} < 0.54$) collisions are shown, as a function of the incident beam energy, in the left panel of fig. 3. The difference of such $\mathrm{v2}_n/\mathrm{v2}_p$ ratios between the stiff and soft choices can be taken as a sensitivity of the proposed observable, and is shown in the right panel of the same figure.

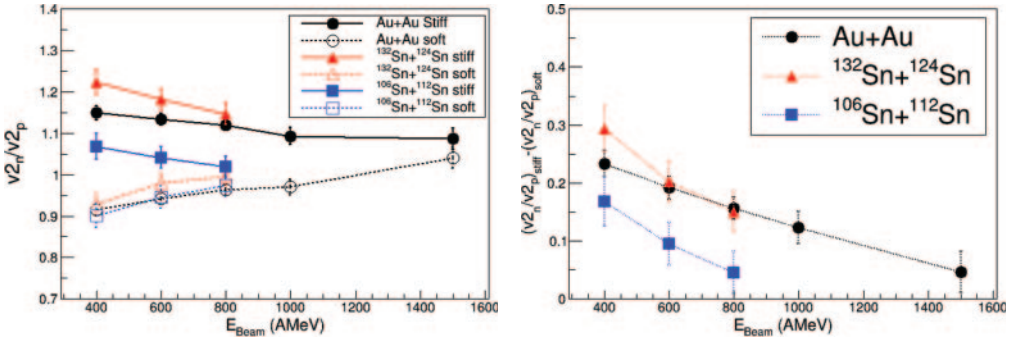

Fig. 3. – Left panel: excitation functions of neutron-to-proton elliptic flow ratios, $v2_n/v2_p$ as predicted by the UrQMD model for stiff and soft $E_{sym}(\rho)$. Right panel: differences between the stiff and soft results. Simulations and results by P. Russotto.

The obtained sensitivity decreases with the beam energy, since the mean-field contribution decreases at higher energies where the two-body collisions start to dominate. Nevertheless, up to 1 AGeV the sensitivity of the proposed observable is 15%, while a measurement can easily reach a 5% accuracy, allowing clear discrimination between stiff and soft choices. It is also important to stress the differences in trends (slopes) observed in the left panel of fig. 3, which by themselves have a discriminating power. For the soft EoS the ratios increase with the energy while for the stiff one the trend is opposite. This proves the needs for measuring the excitation functions of these observables and the importance of using neutron-rich beams where the effect is stronger. In addition, measuring the double Sn + Sn system would allow differential observables to be built which enable to control the Coulomb *vs.* E_{sym} competition and to strongly reduce the model dependencies and systematic errors.

In order to improve the results as compared to the ASY-EOS ones it is necessary to improve the mass resolution of the measured hydrogen isotopes. This seems to be granted by the usage of the NeuLAND detector [62], which would be the main detector measuring neutrons in the first place. Additional charged-particle detectors like KRAB (see below), FOPI Plastic wall [63], KRATTA [64], FARCOS [65] and CALIFA [66] would allow to collect information on centrality, reaction plane, light cluster production, flows and correlations. The systems/energies intended to be measured in the future campaign are: ^{197}Au + ^{197}Au at 400, 600, 1000 AMeV, ^{132}Sn + ^{124}Sn at 400, 600 AMeV and ^{106}Sn + ^{112}Sn at 400, 600 AMeV. The setup requires a detector which would provide a fast trigger, based on the multiplicity threshold and would precisely measure the azimuthal distributions of charged particles beyond the angular acceptance of the FOPI Plastic Wall. A schematic design of such a device is presented below.

9. – KRAB

Taking into account the experimental demands, the current design of the KRAków Barrel, KRAB, detector (see fig. 4) assumes the following features: 5 rings of $4 \times 4\,\mathrm{mm}^2$ fast scintillating fibers (*e.g.*, BCF-10) read out by SiPMs, coverage of polar angles from 30° to 165°, segmentation assuring more or less uniform count rates for the Au + Au at 1 AGeV, geometrical efficiency ∼85% less than 11% of charged particles involved in multi-hits, single segment multi-hit probability less than 5%, sufficiently large entrance

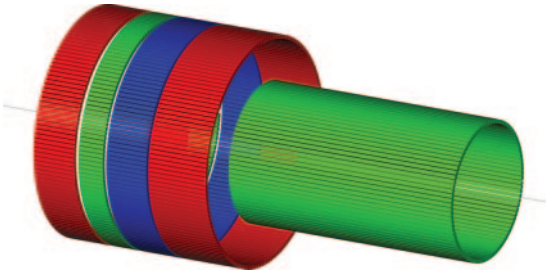

Fig. 4. – Design of the KRAB detector.

for radioactive beams, sufficiently small size and weight not to disturb neutrons, min radius ∼7 cm, max radius ∼ 12 cm, length ∼ 46 cm, 4×160 segments in forward rings, 96 segments in backward ring, 736 channels.

The above preliminary design and properties have been obtained using the GEANT4 simulations with the UrQMD predictions for the Au+Au collisions at 1 AGeV used as an event generator. Based on the predicted multiplicity and angular distributions it was possible to come out with the proposed structure and segmentation. In particular, the simulations indicate that the Barrel should provide better estimates of centrality as compared to the FOPI Plastic Wall. In the first ASY-EOS experiment the target region was covered by the MICRO-BALL [67] detector which was found very useful for providing a veto information for reactions occurring on air and material up-stream of the target. Nevertheless, it was too slow to be used as a trigger (CsI crystals) and had too small segmentation for the multiplicities from the high energy beams. It was also too sensitive to the high energy delta electrons, responsible for false multiplicities.

Based on the experience from the first ASY-EOS campaign the design of the KRAB detectors will try to overcome the observed problems and drawbacks. Thanks to the high granularity, together with the FOPI Plastic Wall it should provide sharp estimates for the orientation of the reaction plane and the unbiased multiplicities. The observed quality of the simulated signals gives rise to the expectation that the device will indeed provide very precise information on the orientation of the reaction plane and on the centrality of the collision. It will also play invaluable role by vetoing the upstream reactions.

The KRAB detector will cover about 85% of the total solid angle. Together with the FOPI Plastic Wall (7%) they will cover almost 92% of the 4π.

Application of the fast plastic scintillator and fast silicon photon counters together with the compact size of the KRAB detector will assure perfect timing, and thus triggering properties and insensitivity to magnetic fields. Compact size should allow to place the device inside bigger ones, such as, *e.g.*, the CALIFA barrel.

Summarizing, we have shown the importance and difficulties of the symmetry energy quest. Some controversies regarding the inference of the NS radius from the qLMXB systems seem to be resolved by the recent interpretations of the first gravitational wave signal. The results from low energy experiments and nuclear data analyses on the stiffness of the symmetry energy (L parameter) are well within the limits imposed by the GW170817 signal and agree within 2σ with the results from the NS radius estimates. The values of L parameter from high energy measurements are generally slightly above the averages from the recent compilations of the data from low density probes. Does it imply a transition to stiffer EoS above the saturation density? Possibly the new planned

experiments will shed some more light on that. Definitely more tight constraints on the symmetry energy, especially at high densities are needed. New missions, new facilities, new experiments and new detectors herald new exciting results in the nearest future.

* * *

Work supported by Polish National Science Centre, contract No. UMO-2017/25/B/ST2/02550.

REFERENCES

[1] Danielewicz P., Lacey R. and Lynch W. G., *Science*, **298** (2002) 1592.
[2] Danielewicz P., arXiv:nucl-th/0512009.
[3] Lattimer J. M. and Prakash M., *Phys. Rep.*, **333** (2000) 121.
[4] Lattimer J. M. and Prakash M., *Astrophys. J.*, **550** (2001) 426.
[5] Li B.-A., Chen L.-W. and Ko C. M., *Phys. Rep.*, **464** (2008) 113.
[6] Abbott B. P. *et al.*, *Phys. Rev. Lett.*, **119** (2017) 161101.
[7] Plagnol E., private communication and `http://sci.esa.int/lisa-pathfinder`.
[8] Bogdanov S., presentation at NUSYM18, `http://nuclear.korea.ac.kr/indico/conferenceDisplay.py?confId=330`, see also `https://www.nasa.gov/nicer`.
[9] Kalogera V. *et al.*, arXiv:astro-ph/0312101v3.
[10] Jhang G. *et al.*, *J. Korean Phys. Soc.*, **69** (2016) 144.
[11] Lasko P. *et al.*, *Nucl. Instrum. Methods A*, **856** (2017) 92.
[12] Isobe T., this conference.
[13] Jhang G., presentation at NUSYM18, `http://nuclear.korea.ac.kr/indico/conferenceDisplay.py?confId=330`.
[14] Kurata-Nishimura M. presentation at NUSYM18, `http://nuclear.korea.ac.kr/indico/conferenceDisplay.py?confId=330`.
[15] Leifels Y. *et al.*, *Phys. Rev. Lett.*, **71** (1993) 963.
[16] Russotto P. *et al.*, *Phys. Lett. B*, **697** (2011) 471.
[17] Russotto P. *et al.*, *Phys. Rev. C*, **94** (2016) 034608.
[18] Li B.-A., *Nucl. Phys. News*, **27** (2017) 7.
[19] Brown B. A., *Phys. Rev. Lett.*, **85** (2000) 5296.
[20] Roca-Maza X. *et al.*, *Phys. Rev. Lett.*, **106** (2011) 252501.
[21] Tsang M. B. *et al.*, *Phys. Rev. C*, **95** (2017) 044614.
[22] Steiner A. W. *et al.*, *Phys. Rep.*, **411** (2005) 325.
[23] Gandolfi S. *et al.*, *Phys. Rev. C*, **85** (2012) 032801(R).
[24] Gandolfi S. and Steiner A. W., *J. Phys. Conf. Ser.*, **665** (2016) 012063.
[25] Fuchs C. and Wolter H. H., *Eur. Phys. J. A*, **30** (2006) 5.
[26] Bao-An Li, *AIP Conf. Proc.*, **1852** (2017) 030005.
[27] Reisdorf W. *et al.*, *Nucl. Phys. A*, **781** (2007) 459.
[28] Xiao Z. *et al.*, *Phys. Rev. Lett.*, **102** (2009) 062502.
[29] Feng Z.-Q. and Jin G.-M., *Phys. Lett. B*, **683** (2010) 140.
[30] Xie W.-J. *et al.*, *Phys. Lett. B*, **718** (2013) 1510.
[31] Jun Xu *et al.*, *Phys. Rev. C*, **93** (2016) 044609.
[32] Guillot S. *et al.*, *Astrophys. J.*, **772** (2013) 7.
[33] Steiner A. W., Lattimer J. M. and Brown E. F., *Astrophys. J. Lett.*, **765** (2013) L5.
[34] Guillot S. and Rutledge R. E., *Astrophys. J. Lett.*, **796** (2014) L3.
[35] Özel F. *et al.*, *Astrophys. J.*, **820** (2016) 28.
[36] Bogdanov S. *et al.*, *Astrophys. J.*, **831** (2016) 184.
[37] Shaw A. W. *et al.*, *Mon. Not. R. Astron. Soc.*, **476** (2018) 4713.
[38] Steiner A. W. *et al.*, *Mon. Not. R. Astron. Soc.*, **476** (2018) 421.
[39] Most E. R. *et al.*, *Phys. Rev. Lett.*, **120** (2018) 261103.
[40] Lim Y. and Holt J. W., *Phys. Rev. Lett.*, **121** (2018) 062701.

[41] Abbott B. P. *et al.*, arXiv:1805.11581 [gr-qc].
[42] De S. *et al.*., *Phys. Rev. Lett.*, **121** (2018) 091102.
[43] Fattoyev F. J. *et al.*, *Phys. Rev. Lett.*, **120** (2018) 172702.
[44] Annala E. *et al.*, *Phys. Rev. Lett.*, **120** (2018) 172703.
[45] Raithel C. A., Özel F. and Psaltis D., *Astrophys. J. Lett.*, **857** (2018) L23.
[46] Bauswein A. *et al.*, *Astrophys. J. Lett.*, **850** (2017) L34.
[47] Lattimer J. M. and Prakash M., *Phys. Rev. Lett.*, **94** (2005) 111101.
[48] Demorest P. B. *et al.*, *Nature*, **467** (2010) 1081.
[49] Lattimer J. M. and Prakash M., *Phys. Rep.*, **442** (2007) 109.
[50] Galloway D. K. *et al.*, *Mon. Not. R. Astron. Soc.*, **387** (2008) 268.
[51] Oertel M. *et al.*, *Rev. Mod. Phys.*, **89** (2017) 015007.
[52] Tsang M. B. *et al.*, *Phys. Rev. Lett.*, **102** (2009) 122701.
[53] Li B. A. and Han X., *Phys. Lett. B*, **727** (2013) 276.
[54] Tsang M. B. *et al.*, *Phys. Rev. C*, **86** (2012) 015803.
[55] Lattimer J. M. and Steiner A. W., *Eur. Phys. J. A*, **50** (2014) 40.
[56] Cozma M. D. *et al.*, *Phys. Rev. C*, **88** (2013) 044912.
[57] Wang Y. *et al.*, *Phys. Rev. C*, **89** (2014) 044603.
[58] Cozma M. D., *Eur. Phys. J. A*, **54** (2018) 40.
[59] Li Q., *J. Phys. G*, **31** (2005) 1359.
[60] Lattimer J. M. and Prakash M., *Phys. Rep.*, **621** (2016) 127.
[61] Li B.-A., *Nucl. Phys. A*, **708** (2002) 365.
[62] `http://www.gsi.de/r3b`.
[63] Gobbi A. *et al.*, *Nucl. Instrum Methods A*, **324** (1993) 156.
[64] Łukasik J. *et al.*, *Nucl. Instrum. Methods A*, **709** (2013) 120.
[65] Pagano E. V. *et al.*, *EPJ Web of Conferences*, **117** (2016) 10008.
[66] Cortina-Gil D. *et al.*, *Nucl. Data Sheets*, **120** (2014) 99.
[67] Sarantites D. G. *et al.*, *Nucl. Instrum. Methods A*, **381** (1996) 418.